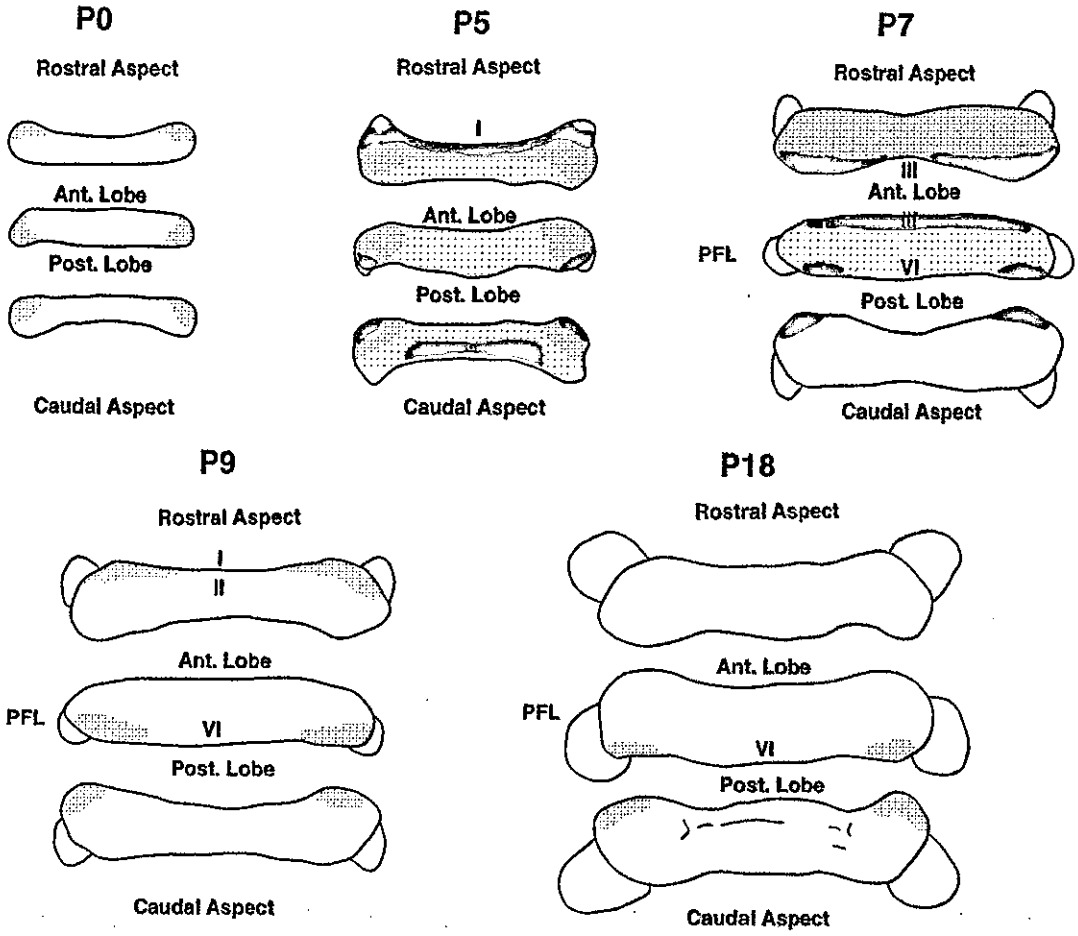

FIG. 7. Distribution of pontocerebellar terminals in weaver mutant mice. Distribution of mossy fibre terminals in the cerebellar cortex of the mutant is summarized in order of age. Stained terminals were counted and described as zonal distributions. Hatching patterns correspond to the densities of terminals: red represents >20 terminals/μm^2, high density spots are 10–20 terminals/μm^2, low density spots are <10 terminals/μm^2 and white represents no terminals. Ant. Lobe, anterior lobe; Post. Lobe, posterior lobe; I, III, VI, lobule I, III, VI, respectively; PFL, paraflocculus.

and weaver mutant mice became more obvious. It was hard to count the number of terminals of mossy fibres in the entire cerebellar cortex of the wild-type mice, due to its extremely high density. In weaver mice, however, instead of an increasing number after P5 a reduction was observed. Even in the hemispheres, fibrous staining patterns were turned to sparsely dotted staining (Fig. 6D). This result suggested that even innervating fibres began to retract from the cortex in the mutant around this stage. After P9, stained fibrous structures were rarely observed in the entire cortex of the mutant, indicating an almost complete degeneration of the afferents at the late stages (Fig. 6E). These results showed that the degeneration of pontocerebellar fibres started early, at the latest at P5, then accelerated until P9 to make almost complete elimination of the afferents from the vermis of mutant cerebellum. The change in distribution patterns of mossy fibre terminals in the mutant is summarized in Fig. 7.

Discussion

In the present study, degeneration of the pontine nuclei in weaver mutant mice was revealed as a decrease in the number of projection neurons and the reductive changes in the shape of the nuclei. Although the degeneration of granule cells in the cerebellum and dopaminergic neurons in the substantia nigra has been extensively studied in the weaver mutant, degeneration of the other brain regions has never been reported. This is the first report showing neuronal cell death in the pontine nuclei in the mutant.

Pontine nuclear neurons were degenerated in weaver mutant mice probably due to direct effect of the GIRK2 mutant gene

There are three possible causes of neuronal death in the pontine nuclei of the mutant. (i) The mutation of the weaver mouse localized in the *GIRK2* gene directly induced the degeneration of pontine nucleus neurons. (ii) Loss of axonal target neurons, i.e. cerebellar granule cells, caused neuronal death of projecting neurons in the pontine nuclei. (iii) Coordination of the previous two causes, i.e. expression of mutated *GIRK2* gene and loss of the axonal target neurons, has strong effects on the survival of the pontine nuclear neurons.

In the weaver mutant, one amino acid substitution (Gly^{156} to Ser) occurrs in the pore region H5 of the GIRK2 subunit of inwardly rectifying K^+ channel (Patil *et al.*, 1995). The mutation results in the formation of the homomeric channels losing their G-protein dependency and ion selectivity to produce constitutive depolarization of expressing neurons (Kofuji *et al.*, 1996; Navarro *et al.*, 1996; Slesinger *et al.*, 1996; Hou *et al.*, 1999). In the pontine nuclei,

expression of *GIRK2* gene starts at the late embryonic stage and continues until adulthood, while the expression of *GIRK1* and *GIRK3* is relatively weak in early developmental stages or starts at a later stage (Kobayashi *et al.*, 1995; Chen *et al.*, 1997; Wei *et al.*, 1997). These results suggest formation of homomeric mutant channels in the pontine nuclear neurons during early postnatal stages, which may cause strong depolarization and cell death of the neurons.

DiI tracing experiments revealed the innervation patterns of pontocerebellar fibres in wild-type and weaver mutant mice during cerebellar development. In early postnatal days (from P0 to P3), it was hard to detect differences in the afferent innervation between wild-type and the mutant mice. After P5, however, the reduction in the number of mossy fibre terminals in cerebellar cortex was evident in the mutant. This phenomenon suggested that the degeneration of pontine nuclear neurons was set out around this stage. On the other hand, in the wild-type mice the number of pontocerebellar afferents is constantly increased during the developmental stage, waiting for the compliment of granule cell movement from the external granular layer to the internal granular layer, but without establishment of stable connections until P14 (Altman & Bayer, 1997). The degeneration in weaver mutants, i.e. retraction of mossy fibres and cell death of pontine nuclear neurons, occurred too early to be caused by loss of connections with their target neurons, i.e. cerebellar granule cells. Considering the time-course of degenerative phenomena in the pontine nuclei, cerebellar cortex and their connections in weaver mutants, it is assumed that the degeneration of pontine nucleus neurons may be caused mainly by their intrinsic properties.

Mossy fibres are categorized in several groups according to their origins. One of them, the spinocerebellar mossy fibre system, has been studied for its behaviour in weaver mutant mice (Sotelo, 1975; Arsenio Nunes *et al.*, 1988). Although the afferents lose their target neurons in the mutant, they interact with Purkinje cells to make heterologous synaptic connections and maintain their inputs to the cerebellar cortex. If pontocerebellar mossy fibres were in the same situation, they could interact with Purkinje cells and maintain the afferents to the cerebellar cortex. However, projection neurons in the pontine nuclei had degenerated and pontocerebellar fibres were eliminated from the cerebellar cortex without making connection with cerebellar neurons. Therefore, the present findings suggest the existence of mechanisms for the strong pontine degeneration which differ from those of other mossy fibre systems, and support the idea that the formation of the homomeric mutant channel directly produces or strongly accelerates degeneration of the pontine nuclear neurons in the weaver mutant.

The loss of pontocerebellar mossy fibres may cause relatively severe degeneration in the central region of weaver mutant cerebellum

In the present study, we observed the neuronal death in the pontine nuclei and the degeneration of pontocerebellar mossy fibres in weaver mutant mice. However, previous studies have shown that the other mossy fibre systems keep their normal structural features in the mutant (Arsenio Nunes *et al.*, 1988; Baurle & Guldin, 1998). From these results, only pontocerebellar fibres (among precerebellar afferents) showed degeneration and retraction from the cerebellar cortex in weaver mutant mice, and this phenomenon correlates well with the relatively strong degeneration of the central and posterior lobes, major projection areas of the pontocerebellar fibres. The results may suggest that the death of projection neurons in the pontine nuclei causes the severe degeneration of the central region of the cerebellar cortex, through elimination of mossy fibres from the region in the mutant.

Previously, Sotelo (1975) has shown that spinocerebellar afferents were connecting with Purkinje cells instead of granule cells to form heterologous synapses in the mutant adult mice. In the anterobasal and anterodorsal lobes, the major terminal field of spinocerebellar fibres, the topographic map of the afferents was almost normal in the mutant, although mossy fibres lost their target neurons (Arsenio Nunes *et al.*, 1988). From these results, Sotelo and colleagues proposed that the connections of mossy fibres with Purkinje cells, as well as granule cells, might be important for cerebellar cortical development (Sotelo, 1990; Sotelo & Wassef, 1991). Recently, with the DiI tracing method, we observed transient direct interaction between pontocerebellar fibres and Purkinje cells during the early postnatal stage of the cerebellum in normal mice. The interactions between mossy fibres and Purkinje cells in developing cerebellum were also observed with HRP injection and electrophysiological methods (Mason & Gregory, 1984; Takeda & Maekawa, 1989). In the present study, we found no obvious connections of pontocerebellar fibres with Purkinje cells during development of weaver mutant mice. Unlike in the the anterior region, pontocerebellar fibres have never directly connected with Purkinje cells in the central region in weaver mutant, correlating with severe degeneration of the region. The relatively normal formation of lobular structures in the anterior and posterior regions in spite of the degeneration of granule cells may depend on the direct interaction between mossy fibres and Purkinje cells in weaver mutant mice. The present results support the hypothesis that direct connections between mossy fibres and Purkinje cells, as well as granule cells, is important for formation and compartmentation of cerebellar cortex during development.

Acknowledgements

We thank Dr R. T. Kado for critically reading the manuscript. This study was supported in part by Grant-in-Aid for Encouragement of Young Scientists from the Ministry of Education, Culture Sports, Science and Technology, Japan (to M.O.)

Abbreviations

E, embryonic day; P, postnatal day.

References

Altman, J. & Bayer, S.A. (1997) *Development of the Cerebellar System: in Relation to its Evolution, Structure, and Functions*. CRC Press, New York.

Arsenio Nunes, M.L., Sotelo, C. & Wehrle, R. (1988) Organization of spinocerebellar projection map in three types of agranular cerebellum: Purkinje cells vs. granule cells as organizer element. *J. Comp. Neurol.*, **273**, 120–136.

Baurle, J. & Guldin, W. (1998) Vestibular ganglion neurons survive the loss of their cerebellar targets. *Neuroreport*, **9**, 4119–4122.

Chen, S.C., Ehrhard, P., Goldowitz, D. & Smeyne, R.J. (1997) Developmental expression of the GIRK family of inward rectifying potassium channels: implications for abnormalities in the weaver mutant mouse. *Brain Res.*, **778**, 251–264.

Eisenman, L.M. (2000) Antero-posterior boundaries and compartments in the cerebellum: evidence from selected neurological mutants. In Gerrits, N.M., Ruigrok, T.J.H. & Zeeuw, C.I.D. (eds), *Cerebellar Modules: Molecules, Morphology and Function*, **Vol. 124**. Elsevier, Amsterdam, pp. 23–30.

Eisenman, L.M., Gallagher, E. & Hawkes, R. (1998) Regionalization defects in the weaver mouse cerebellum. *J. Comp. Neurol.*, **394**, 431–444.

Herrup, K. (1996) The weaver mouse: a most cantankerous rodent [comment]. *Proc. Natl Acad. Sci. USA*, **93**, 10541–10542.

Herrup, K. & Kuemerle, B. (1997) The compartmentalization of the cerebellum. *Annu. Rev. Neurosci.*, **20**, 61–90.

Hess, E.J. (1996) Identification of the weaver mouse mutation: the end of the beginning. *Neuron*, **16**, 1073–1076.

Hou, P., Yan, S., Tang, W. & Nelson, D.J. (1999) The inwardly rectifying K (+) channel subunit GIRK1 rescues the GIRK2 weaver phenotype. *J. Neurosci.*, **19**, 8327–8336.

Kobayashi, T., Ikeda, K., Ichikawa, T., Abe, S., Togashi, S. & Kumanishi, T. (1995) Molecular cloning of a mouse G-protein-activated K+ channel (mGIRK1) and distinct distributions of three GIRK (GIRK1, 2 and 3) mRNAs in mouse brain. *Biochem. Biophys. Res. Commun*, **208**, 1166–1173.

Kobayashi, T., Ikeda, K., Kojima, H., Niki, H., Yano, R., Yoshioka, T. & Kumanishi, T. (1999) Ethanol opens G-protein-activated inwardly rectifying K+ channels. *Nature Neurosci.*, **2**, 1091–1097.

Kofuji, P., Hofer, M., Millen, K.J., Millonig, J.H., Davidson, N., Lester, H.A. & Hatten, M.E. (1996) Functional analysis of the weaver mutant GIRK2 K+ channel and rescue of weaver granule cells. *Neuron*, **16**, 941–952.

Mason, C.A. & Gregory, E. (1984) Postnatal maturation of cerebellar mossy and climbing fibers: transient expression of dual features on single axons. *J. Neurosci.*, **4**, 1715–1735.

Navarro, B., Kennedy, M.E., Velimirovic, B., Bhat, D., Peterson, A.S. & Clapham, D.E. (1996) Nonselective and G betagamma-insensitive weaver K+ channels. *Science*, **272**, 1950–1953.

Ozaki, M., Hashikawa, T. & Yano, R. (1999) The connection between granule cells and mossy fibers changes dynamically during postnatal cerebellar development. In Uyemura, K., Kawamura, K. & Yazaki, T. (eds), *Neural Development*, **Vol. 2**. Springer-Verlag, Tokyo, pp. 425–429.

Patil, N., Cox, D.R., Bhat, D., Faham, M., Myers, R.M. & Peterson, A.S. (1995) A potassium channel mutation in weaver mice implicates membrane excitability in granule cell differentiation [see comments]. *Nature Genet.*, **11**, 126–129.

Rakic, P. & Sidman, R.L. (1973a) Organization of cerebellar cortex secondary to deficit of granule cells in weaver mutant mice. *J. Comp. Neurol.*, **152**, 133–161.

Rakic, P. & Sidman, R.L. (1973b) Sequence of developmental abnormalities leading to granule cell deficit in cerebellar cortex of weaver mutant mice. *J. Comp. Neurol.*, **152**, 103–132.

Ruigrok, T.J.H. & Cella, F. (1995) Precerebellar nuclei and red nucleus. In Paxinos, G. (ed.), *The Rat Nervous System*. Academic Press, San Diego, pp. 277–308.

Slesinger, P.A., Patil, N., Liao, Y.J., Jan, Y.N., Jan, L.Y. & Cox, D.R. (1996) Functional effects of the mouse weaver mutation on G protein-gated inwardly rectifying K+ channels. *Neuron*, **16**, 321–331.

Sotelo, C. (1975) Anatomical, physiological and biochemical studies of the cerebellum from mutant mice. II. Morphological study of cerebellar cortical neurons and circuits in the weaver mouse. *Brain Res.*, **94**, 19–44.

Sotelo, C. (1990) Cerebellar synaptogenesis: what we can learn from mutant mice. *J. Exp. Biol.*, **153**, 225–249.

Sotelo, C. & Wassef, M. (1991) Cerebellar development: afferent organization and Purkinje cell heterogeneity. *Phil. Trans. R. Soc. Lond. B Biol. Sci.*, **331**, 307–313.

Takeda, T. & Maekawa, K. (1989) Transient direct connection of vestibular mossy fibers to the vestibulocerebellar Purkinje cells in early postnatal development of kittens. *Neuroscience*, **32**, 99–111.

Voogd, J. (1995) Cerebellum. In Paxinos, G. (ed.), *The Rat Nervous System*. Academic Press, San Diego, pp. 309–350.

Wei, J., Dlouhy, S.R., Bayer, S., Piva, R., Verina, T., Wang, Y., Feng, Y., Dupree, B., Hodes, M.E. & Ghetti, B. (1997) In situ hybridization analysis of Girk2 expression in the developing central nervous system in normal and weaver mice. *J. Neuropathol. Exp. Neurol.*, **56**, 762–771.

6

Opioid Receptor Coupling to GIRK Channels

In Vitro Studies Using a Xenopus *Oocyte Expression System and In Vivo Studies on* Weaver *Mutant Mice*

Kazutaka Ikeda, Mitsunobu Yoshii, Ichiro Sora, and Toru Kobayashi

1. Introduction

Opioid receptors are coupled to a variety of effectors, including G protein-activated inwardly rectifying potassium (GIRK) channels (also known as Kir3), adenylyl cyclases, and voltage-dependent calcium channels *(1)*. GIRK channels have been shown to be involved in opioid-induced analgesia *(2)*. These channels are activated by G protein-coupled receptors (GPCRs) such as opioid, nociceptin/orphanin FQ, M2 muscarinic, α_2 adrenergic, and D_2 dopaminergic receptors via the $\beta\gamma$ subunits of G proteins ($G\beta\gamma$) (*see* **Fig. 1**) *(3–7)*. Activation of GIRK channels induces membrane hyperpolarization of the neurons via efflux of potassium ions, ultimately reducing neural excitability and heart rate *(3,8–10)*. GIRK channels are members of a family of inwardly rectifying potassium (IRK) channels which have two transmembrane regions and one pore-forming region (*see* **Fig. 2**). The cDNAs for four GIRK channel subunits have been cloned from mammalian tissues *(11–13)*. Neuronal GIRK channels in most regions of the central nervous system (CNS) are predominant heteromultimers consisting of GIRK1 and GIRK2 subunits *(14–16)*, whereas atrial GIRK channels are heteromultimers consisting of GIRK1 and GIRK4 subunits *(17)*. The GIRK1, GIRK2, and GIRK3 subunits are widely and distinctively expressed in the CNS *(14,16,18)*, suggesting that they are involved in diverse functions of the CNS such as cognition, memory, emotion, and motor coordination. In many neurons, GIRK channels are coexpressed with opioid receptors *(6)*. For investigation of opioid-receptor

From: *Methods in Molecular Medicine, Vol. 84: Opioid Research: Methods and Protocols*
Edited by: Z. Z. Pan © Humana Press Inc., Totowa, NJ

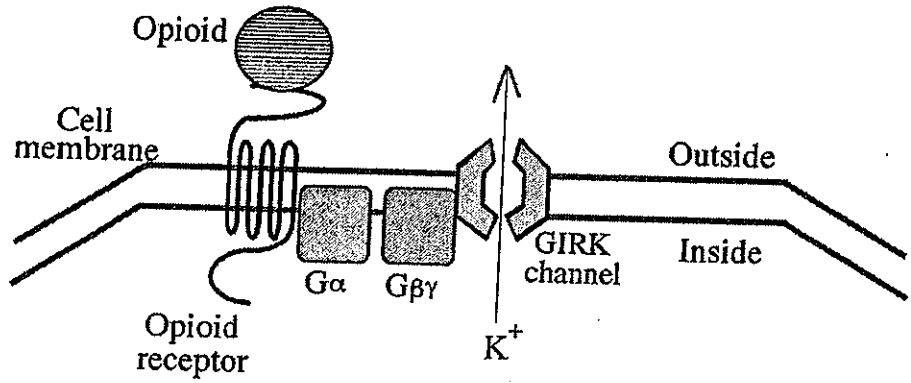

Fig. 1. Schematic drawing of opioid receptor and GIRK channel coupling.

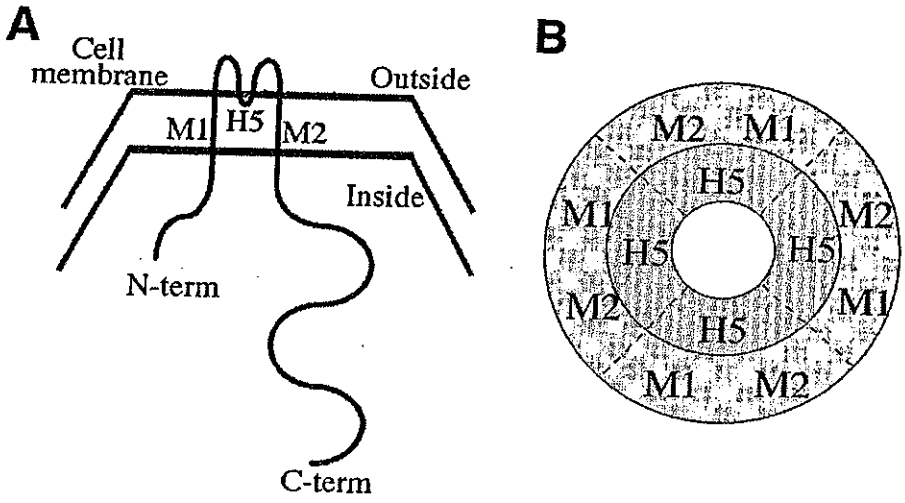

Fig. 2. Schematic drawings of a GIRK channel. **(A)** Schematic drawing of GIRK subunit structure. **(B)** Schematic drawing of GIRK channel structure. A GIRK channel is composed of 4 GIRK subunits. M1, M2: transmembrane domains 1, 2. H5: pore-forming region.

functions in vitro, especially coupling of opioid receptors to GIRK channels, the *Xenopus* oocyte expression system is sensitive and valuable in generating functional analyses and physiological significance. Functions of the opioid system, including analgesia and reward, can be analyzed only in animals, not in individual cells. The *weaver* mutant mouse serves as an ideal animal model for studying the role of the GIRK channel in vivo because of the impaired couplings of opioid receptors to GIRK channels *(19)*.

2. Materials

1. First strand cDNA (e.g., mouse brain cDNA).
2. Expression vector [e.g., pSP35T *(20)* (*see* **Fig. 3**)].

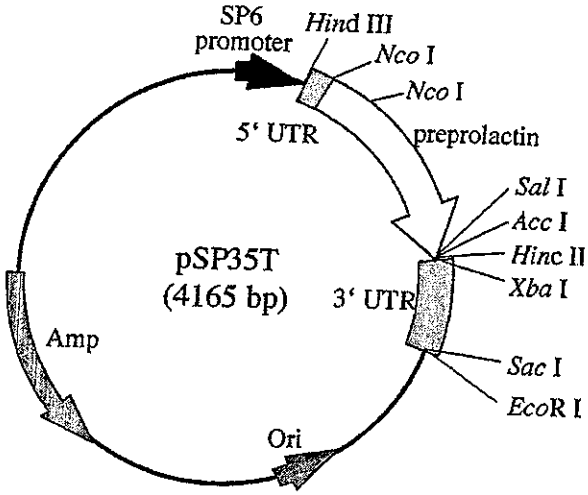

Fig. 3. Schematic drawing of pSP35T expression plasmid. 5' UTR: the 5' untranslated region of *Xenopus* β-globin. 3' UTR: the 3' untranslated region of *Xenopus* β-globin. Preprolactin can be substituted by cDNA for receptor or channel. Amp: ampicillin resistant gene. Ori: origin of replication.

3. DNA polymerase (e.g., *Pfu* DNA polymerase; Stratagene; La Jolla, CA).
4. mRNA synthesis kit (e.g., mMESSAGEmMACHINE; Ambion, Austin, TX).
5. STE solution: 150 m*M* NaCl, 10 m*M* Tris-HCl, pH 7.5, 1 m*M* EDTA.
6. cDNA spun column (e.g., Sephacryl S-300; Amersham Pharmacia Biotech, Buckinghamshire, U.K.).
7. Adult female South African clawed frogs (*Xenopus laevis*) (e.g., Copacetic, Aomori, Japan).
8. 100X Tris-Calcium Solution: 750 m*M* Tris-HCl, pH 7.4, 33 m*M* $Ca(NO_3)_2$, 41 m*M* $CaCl_2$ (Autoclaved).
9. Calcium-free ND96 solution: 96 m*M* NaCl, 2 m*M* KCl, 2 m*M* $MgCl_2$, 5 m*M* HEPES, adjust pH to 7.5 with NaOH.
10. 50X Salts Solution: 4.4 M NaCl, 50 m*M* KCl, 41 m*M* $MgSO_4$ (Autoclaved).
11. Gentamicin sulfate (e.g., Wako Pure Chemical Industries, Ltd., Osaka, Japan).
12. Barth's solution: 1 X Tris-Calcium Solution, 1x Salts Solution, 2.4 m*M* $NaHCO_3$, 0.1 mg/mL gentamicin in autoclaved distilled water.
13. Electrode puller (e.g., PN-3; Narishige, Tokyo, Japan).
14. Microforge (e.g., MF-83; Narishige, Tokyo, Japan).
15. Microinjector (e.g., IM-50B; Narishige, Tokyo, Japan; and Nano liter injector A203XVY model; World Precision Instruments, Inc., Sarasota, FL).
16. Collagenase (e.g., Collagenase Type I; Wako Pure Chemical Industries, Ltd., Osaka, Japan).
17. Perfusion medium, e.g., high potassium solution (HKS): 96 m*M* KCl, 2 m*M* NaCl, 1 m*M* $MgCl_2$, 1.5 m*M* $CaCl_2$.
18. Electrophysiological setup for two-microelectrode voltage clamp.
19. *Weaver* mutant mice (The Jackson Laboratory, Bar Harbor, ME, or our laboratory for C3H-backcrossed mice).

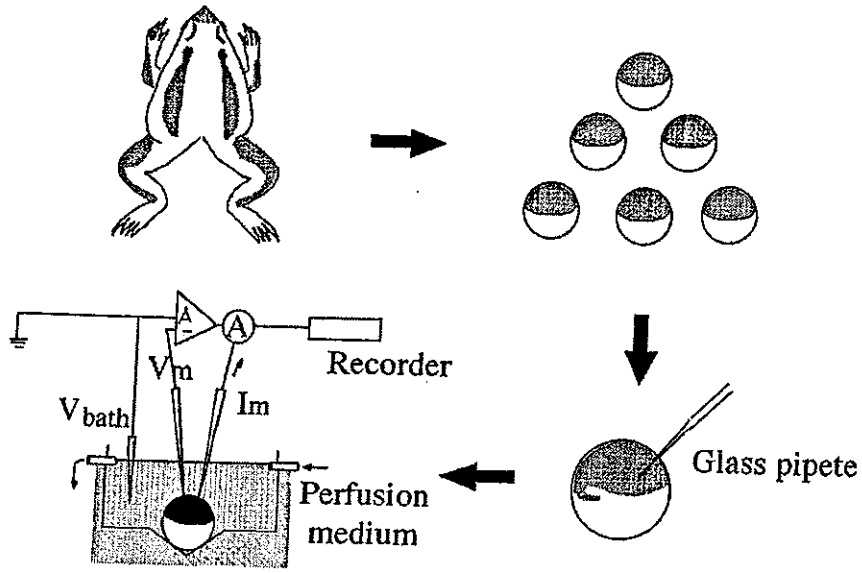

Fig. 4. Experimental procedure for the *Xenopus* oocyte expression system. A: amplifier.

20. Tail-flick test apparatus (e.g., MK-330B; Muromachi Kikai Co., Ltd., Tokyo, Japan).
21. Hot-plate test apparatus (e.g., MK-350B; Muromachi Kikai Co., Ltd.).
22. Open-field test apparatus (e.g., X-Y-Z; Muromachi Kikai Co., Ltd., Tokyo, Japan).
23. Morphine chloride.
24. (–)–U50488 hydrochloride.

3. Methods

3.1. Xenopus Oocyte Expression System (see Fig. 4)

Xenopus laevis oocytes have been widely used in studies on the function and regulation of a variety of ion channels and receptors *(21)*. They are unfertilized eggs that install all biochemical machinery necessary for translating mRNA, for transporting the resulting protein, and for inserting it correctly in the plasma membrane *(22)*. Detailed understanding of the physiological characteristics of oocyte plasma membrane has enabled the characterization of proteins translated from foreign mRNAs *(22)*. *Xenopus* oocytes possess an endogenous GIRK subunit (XIR) which forms a heteromultimer channel with an exogenously expressed GIRK1 subunit *(23,24)*. No endogenous opioid receptor has been found in *Xenopus* oocytes. The *Xenopus* oocyte expression system is superior to ligand binding methods because it allows the activation and inhibition of receptors to be studied under physiological conditions *(25,26)*.

Sensitivity of the system is superior to conventional ligand binding methods and cAMP accumulation methods. Because opioid receptors are functionally coupled to GIRK channels via Gi/o proteins, investigations using the *Xenopus* oocyte expression system with these molecules should provide more physiologically relevant information than the Fluorometric Imaging Plate Reader (FLIPR) system with Gi/Gq chimeric G proteins *(27)*.

3.1.1. Construction of Expression Vectors

The pSP35T (*see* **Fig. 3**) expression system developed by Amaya *(20)* is highly effective in producing recombinant receptors and channels (e.g., mu-opioid receptor and GIRK channel) in *Xenopus* oocytes. This is because it contains those nucleotide sequences that correspond to the untranslated regions of *Xenopus* oocyte β-globin mRNA. Other expression vectors can also be used (e.g., pBKSA) *(28)* (*see* **Note 1**). The procedure is as follows:

1. Synthesize the first strand cDNA using template mRNA (e.g., mouse brain mRNA).
2. Synthesize a pair of oligonucleotide primers containing nucleotide sequences corresponding to the initiating methionine and stop codon. In the case of pSP35T vector, preferable sites for recombination are *Nco* I and *Xba* I sites (*see* **Note 2**).
3. Amplify the cDNA for the receptor or channel by PCR with *Pfu* DNA polymerase, with the first strand cDNA as a template and with the primers.
4. Insert the cDNA at the appropriate site of the pSP35T vector (*see* **Note 3**).
5. Amplify the recombinant vector plasmid using *Escherichia coli*.
6. Purify the plasmid (e.g., Qiagen plasmid purification kit).
7. Linearize the plasmid with an appropriate restriction enzyme (*Eco*R I or *Sac* I in the case of pSP35T).
8. Purify the linearized plasmid with conventional phenol/chloroform treatment.
9. Dissolve the plasmid with RNase-free distilled water at 0.5 mg/mL.

3.1.2. mRNA Synthesis

1. Synthesize mRNA using an RNA synthesis kit (e.g., mMESSAGEmMACHINE) with the linearized plasmid as template.
2. Degrade the template DNA with RNase-free DNase I.
3. Purify the mRNA with conventional phenol/chloroform treatment.
4. Remove chloroform completely by diethylether treatment (twice).
5. Purify the mRNA by gel-chromatography using cDNA spun columns buffered with STE solution.
6. Measure the mRNA concentration.
7. Add 1/19 vol of 3 *M* sodium acetate.
8. Add 2.5 vol of ethanol.
9. Store at –80°C.

Figure 5. *Xenopus* oocytes. Left, oocytes inappropriate for experiment. These are too small or dying. Right, mature oocytes (Stage V and VI) as used in experiments. It is useful to leave a small amount of connective tissue or follicle cell layer surrounding the oocytes for removal of the follicle cell layer after collagenase treatment.

3.1.3. Oocyte Preparation

1. Maintain adult female South African clawed frogs at 19°C (*see* **Note 4**).
2. Anesthetize the frog by immersion in water containing 0.15% tricaine.
3. Remove several ovarian lobes from the abdomen, and immerse these in Barth's solution.
4. Isolate mature oocytes suitable for experiments, using spring scissors and forceps (*see* **Fig. 5**).

3.1.4. Injection and Collagenase Treatment

1. Prepare injection pipets from glass tubes using a puller, a microforge (*see* **Fig. 6**) and a sterilizing oven (200°C for 8 h).
2. Centrifuge an appropriate volume of mRNA(s) (ethanol suspension) and remove the supernatant.
3. Dissolve the mRNA(s) in 10 µL distilled water (approx 10 pmol/mL).
4. Inject the mRNA solution into approx 100 oocytes using the glass pipet and the microinjector.
5. Incubate the injected oocytes in Barth's solution for 2 d at 19°C.
6. Treat the oocytes with collagenase (1 mg/mL) dissolved in calcium-free ND96 solution for 1 h at 19°C.
7. Remove the follicle cell layer from the oocytes using forceps and maintain the oocytes in Barth's solution.

3.1.5. Voltage Clamp Recording

1. Prepare HKS or other perfusion medium.
2. Fill the micropipet electrode with 3 *M* KCl. The resistance of the current-injecting

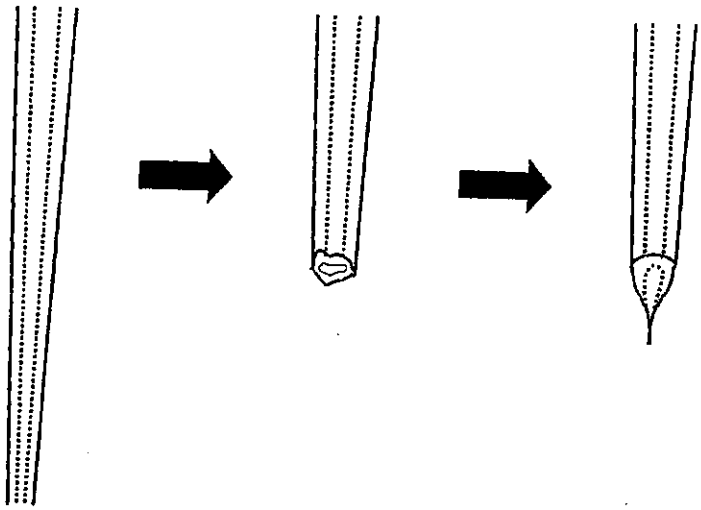

Fig. 6. Preparation of injection pipets. A glass pipet is prepared using the puller. After breaking off the pipet tip, the shape of the tip is changed using a microforge.

electrode (*Im*) should be approx 1 *MΩ* and the resistance of the potential electrode (*Vm*) approx 5 MΩ.

3. Measure the bath potential (*V*bath) with the potential electrode and adjust it to zero.
4. Insert the potential electrode into the oocyte using a micromanipulator and measure the resting potential.
5. Insert the current electrode. Clamp the membrane at –70 mV and wait until the current becomes stable (*see* **Note 5**).
6. Apply drugs to perfusion medium in sequence and record the membrane currents as responses to the drugs (*see* **Note 6**).

3.2. Weaver *Mutant Mice*

To understand actions of the opioid system in vivo, including analgesia, euphoria, and dependence, animal experiments are necessary. The *weaver* mutant mouse is a valuable animal model because the coupling of opioid receptors to GIRK channels is impaired and no specific activators or blockers of GIRK channels has yet been found. The mutant mice possess a missense point mutation in the pore-forming region of the GIRK2 subunit *(29)* (*see* **Fig. 7**). The activity of the mutant GIRK channel is not regulated by G proteins *(19)*, implying that the pathway of opioid signaling via GIRK channels is impaired in weaver mutant mice. Interestingly, *weaver* mutant mice show reduced analgesia after administration of either morphine or kappa-opioid receptor agonists *(30)*, although a nonsteroidal antiinflammatory drug (NSAID) induces analgesia normally *(31)*. These results suggest the involvement of GIRK channels in opioid-induced analgesia. Further investigation using *weaver* mutant mice promises a better understanding of opioid functions in vivo.

Wild type	ACA	GAA	ACC	ACC	ATC	GGT	TAT	GGC	TAC	CGG
	Thr	Glu	Thr	Thr	Ile	Gly	Tyr	Gly	Tyr	Arg
Weaver	ACA	GAA	ACC	ACC	ATC	AGT	TAT	GGC	TAC	CGG
	Thr	Glu	Thr	Thr	Ile	Ser	Tyr	Gly	Tyr	Arg
Amino-acid No.	151	152	153	154	155	156	157	158	159	160

Fig. 7. A missense point mutation in a gene encoding the GIRK2 subunit in *weaver* mutant mice.

Fig. 8. Testes of C3H (left) and *weaver* mutant (right) mice.

3.2.1. Breeding

Weaver mutant mice with genetic background C57BL/6 can be purchased from the Jackson Laboratory. Breeding of the homozygous mice is difficult due to impaired testicular development (*see* **Fig. 8**). Homozygous mutant mice can be obtained efficiently by mating heterozygous male and homozygous female mice. Homozygous *weaver* mutant mice with genetic background C3H are readily bred ***(31)*** (*see* **Note 7**).

3.2.2. Genotyping

1. Cut the tip (approx 5 mm) of the mouse tail.
2. Prepare the genomic DNA by conventional methods.
3. Amplify the DNA fragment using the PCR method with the following pair of primers:
   5'-ATGATCTGGTGGCTGATTGC-3', 5'-TTGGGATATTTTCACAAACA-3'
4. Analyze the nucleotide sequence of the DNA fragment (*see* **Fig. 7**).

3.2.3. Behavioral Analyses

Opioid-induced analgesia can be evaluated by the tail-flick test or the hot-plate test *(30)*. Examination of locomotor activity is necessary when analyzing the behavior of the *weaver* mutant mouse because these mice display motor ataxia and hyperactivity. Experiments should also be carefully designed (*see* **Note 8**).

4. Notes

1. Either receptors or channels can be expressed in the cell membrane of *Xenopus* oocytes using vector systems possessing appropriate promoters (e.g., pCDNA) when the vectors are injected in the nuclei of oocytes *(32)*. The size of the nucleus is approx one-fourth of the oocyte diameter.
2. It is recommended that GC sequence is added at the 5' end of each nucleotide oligomer. The sequence can be removed when the PCR fragment is digested with restriction enzyme.
3. If recombination of the vector at the *Nco* I site is difficult, a cDNA fragment can be connected at *Hind* III site (removal of the 5' untranslated region of β-globin mRNA), although the amount of expression will be reduced.
4. It is known that stretch activated channels are expressed in *Xenopus* oocytes when the frogs are kept in a warm room. The stretch activated channels make the experiments more difficult.
5. If the holding current does not stabilize within approx 10 min, the oocyte should be discarded.
6. Oocytes can be analyzed several times if they are incubated in Barth's solution after each analysis.
7. Mashed food is better for raising homozygous *weaver* mutant mice. The floor chip in the cage should not be changed during the first week after birth.
8. In weaver mutant mice, neuronal degeneration is observed in the granule cell layer of the cerebellum, the substantia nigra and the pontine nucleus *(33)*. *Weaver* mouse brain is shown in **Fig. 9**.

Acknowledgments

This work was supported by a research grant from the Cooperative Research Program of the RIKEN Brain Science Institute, by Grants-in-Aid for Encouragement of Young Scientists (A), Scientific Research (B) and Scientific Research on Priority Areas (A) and (C) from the Ministry of Education, Culture, Sports, Science and Technology of Japan, by Health Sciences Research Grants (Research on Brain Science and Research on Pharmaceutical and Medical Safety) from the Ministry of Health, Labour and Welfare and by a grant from Nakayama Foundation for Human Science. The authors thank Dr. Enrique Amaya for his kind permission to describe pSP35T in this manuscript. We are

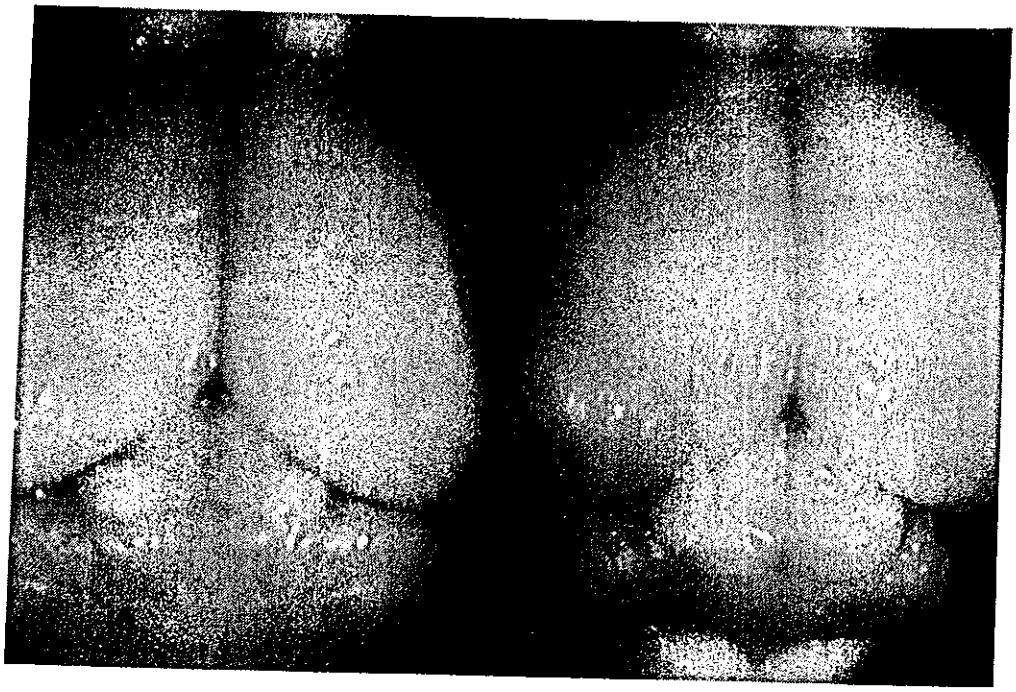

Fig. 9. Brains of C3H (left) and *weaver* mutant (right) mice.

also grateful to Tomio Ichikawa, Naomi Mihira, Yukio Takamatsu, Harumi Hata, Takehiro Takahashi, and Kana Miyahira for their cooperation.

References

1. Law, P. Y., Wong, Y. H., and Loh, H. H. (2000) Molecular mechanisms and regulation of opioid receptor signaling. *Annu. Rev. Pharmacol. Toxicol.* **40,** 389–430.
2. Ikeda, K., Kobayashi, T., Kumanishi, T., Yano, R., Sora, I., and Niki, H. (2002) Molecular mechanisms of analgesia induced by opioids and ethanol: is the GIRK channel the key? *Neurosci. Res.* **44,** 121–131.
3. North, R. A. (1989) Drug receptors and the inhibition of nerve cells. *Br. J. Pharmacol.* **98,** 13–28.
4. Takao, K., Yoshii, M., Kanda, A., Kokubun, S:, and Nukada, T. (1994) A region of the muscarinic-gated atrial K^+ channel critical for activation by G protein beta gamma subunits. *Neuron* **13,** 747–755.
5. Ikeda, K., Kobayashi, K., Kobayashi, T., Ichikawa, T., Kumanishi, T., Kishida, H., et al. (1997) Functional coupling of the nociceptin/orphanin FQ receptor with the G-protein-activated K^+ (GIRK) channel. *Brain Res Mol. Brain Res.* **45,** 117–126.
6. Ikeda, K., Kobayashi, T., Ichikawa, T., Usui, H., Abe, S., and Kumanishi, T. (1996) Comparison of the three mouse G-protein-activated K^+ (GIRK) channels and functional couplings of the opioid receptors with the GIRK1 channel. *Ann. NY Acad. Sci.* **801,** 95–109.
7. Ikeda, K., Kobayashi, T., Ichikawa, T., Usui, H., and Kumanishi, T. (1995) Functional couplings of the d- and the k-opioid receptors with the G-protein-activated K^+ channel. *Biochem. Biophys. Res. Commun.* **208,** 302–308.

8. Brown, A. M. and Birnbaumer, L. (1990) Ionic channels and their regulation by G protein subunits. *Annu. Rev. Physiol.* **52,** 197–213.
9. Signorini, S., Liao, Y. J., Duncan, S. A., Jan, L. Y., and Stoffel, M. (1997) Normal cerebellar development but susceptibility to seizures in mice lacking G protein-coupled, inwardly rectifying K^+ channel GIRK2. *Proc. Natl. Acad. Sci. USA* **94,** 923–927.
10. Wickman, K., Nemec, J., Gendler, S. J., and Clapham, D. E. (1998) Abnormal heart rate regulation in GIRK4 knockout mice. *Neuron* **20,** 103–114.
11. Kubo, Y., Reuveny, E., Slesinger, P. A., Jan, Y. N., and Jan, L. Y. (1993) Primary structure and functional expression of a rat G-protein-coupled muscarinic potassium channel. *Nature* **364,** 802–806.
12. Doupnik, C. A., Davidson, N., and Lester, H. A. (1995) The inward rectifier potassium channel family. *Curr. Opin. Neurobiol.* **5,** 268–277.
13. Reimann, F. and Ashcroft, F. M. (1999) Inwardly rectifying potassium channels. *Curr. Opin. Cell Biol.* **11,** 503–508.
14. Kobayashi, T., Ikeda, K., Ichikawa, T., Abe, S., Togashi, S., and Kumanishi, T. (1995) Molecular cloning of a mouse G-protein-activated K^+ channel (mGIRK1) and distinct distributions of three GIRK (GIRK1, 2 and 3) mRNAs in mouse brain. *Biochem. Biophys. Res. Commun.* **208,** 1166–1173.
15. Lesage, F., Guillemare, E., Fink, M., Duprat, F., Heurteaux, C., Fosset, M., et al. (1995) Molecular properties of neuronal G-protein-activated inwardly rectifying K^+ channels. *J. Biol. Chem.* **270,** 28,660–28,667.
16. Liao, Y. J., Jan, Y. N., and Jan, L. Y. (1996) Heteromultimerization of G-protein-gated inwardly rectifying K^+ channel proteins GIRK1 and GIRK2 and their altered expression in weaver brain. *J Neurosci* **16,** 7137–7150.
17. Krapivinsky, G., Gordon, E. A., Wickman, K., Velimirovic, B., Krapivinsky, L., and Clapham, D. E. (1995) The G-protein-gated atrial K^+ channel IKACh is a heteromultimer of two inwardly rectifying K^+-channel proteins. *Nature* **374,** 135–141.
18. Karschin, C., Dissmann, E., Stuhmer, W., and Karschin, A. (1996) IRK(1-3) and GIRK(1-4) inwardly rectifying K^+ channel mRNAs are differentially expressed in the adult rat brain. *J. Neurosci.* **16,** 3559–3570.
19. Navarro, B., Kennedy, M. E., Velimirovic, B., Bhat, D., Peterson, A. S., and Clapham, D. E. (1996) Nonselective and Gβγ-insensitive weaver K^+ channels. *Science* **272,** 1950–1953.
20. Amaya, E., Musci, T. J., and Kirschner, M. W. (1991) Expression of a dominant negative mutant of the FGF receptor disrupts mesoderm formation in *Xenopus* embryos. *Cell* **66,** 257–270.
21. Dascal, N. (1987) The use of *Xenopus* oocytes for the study of ion channels. *CRC Crit. Rev. Biochem.* **22,** 317–387.
22. Fraser, S. P. and Djamgoz, M. B. A. (1992) *Xenopus* oocytes: endogenous electrophysiological characteristics, in *Current Aspects of the Neurosciences*, (Osborne, N. N., ed.), Macmillan Basingstoke, Hampshire, UK, vol. 4, pp. 267–315.
23. Duprat, F., Lesage, F. Guillemare, E., Fink, M., Hugnot, J. P., Bigay, J., et al. (1995) Heterologous multimeric assembly is essential for K^+ channel activity of

neuronal and cardiac G-protein-activated inward rectifiers. *Biochem. Biophys. Res. Commun.* **212,** 657–663.

24. Hedin, K. E., Lim, N. F., and Clapham, D. E. (1996) Cloning of a *Xenopus laevis* inwardly rectifying K^+ channel subunit that permits GIRK1 expression of IKACh currents in oocytes. *Neuron* **16,** 423–429.
25. Kobayashi, T., Ikeda, K., Ichikawa, T., Togashi, S., and Kumanishi, T. (1996) Effects of sigma ligands on the cloned μ-, δ- and κ-opioid receptors co-expressed with G-protein-activated K^+ (GIRK) channel in *Xenopus* oocytes. *Br. J. Pharmacol.* **119,** 73–80.
26. Kobayashi, T., Ikeda, K., and Kumanishi, T. (1998) Effects of clozapine on the δ- and κ-opioid receptors and the G-protein-activated K^+ (GIRK) channel expressed in *Xenopus* oocytes. *Br. J. Pharmacol.* **123,** 421–426.
27. Coward, P., Wada, H. G., Falk, M. S., Chan, S. D., Meng, F., Akil, H., and Conklin, B. R. (1998) Controlling signaling with a specifically designed Gi-coupled receptor. *Proc. Natl. Acad. Sci. USA* **95,** 352–357.
28. Yamazaki, M., Mori, H., Araki, K., Mori, K. J., and Mishina, M. (1992) Cloning, expression and modulation of a mouse NMDA receptor subunit. *FEBS Lett.* **300,** 39–45.
29. Patil, N., Cox, D. R., Bhat, D., Faham, M., Myers, R. M., and Peterson, A. S. (1995) A potassium channel mutation in *weaver* mice implicates membrane excitability in granule cell differentiation. *Nat. Genet.* **11,** 126–129.
30. Ikeda, K., Kobayashi, T., Kumanishi, T., Niki, H., and Yano, R. (2000) Involvement of G-protein-activated inwardly rectifying K^+ (GIRK) channels in opioid-induced analgesia. *Neurosci. Res.* **38,** 113–116.
31. Kobayashi, T., Ikeda, K., Kojima, H., Niki, H., Yano, R., Yoshioka, T., and Kumanishi, T. (1999) Ethanol opens G-protein-activated inwardly rectifying K^+ channels. *Nat. Neurosci.* **2,** 1091–1097.
32. Swick, A. G., Janicot, M., Cheneval-Kastelic, T., McLenithan, J. C., and Lane, M. D. (1992) Promoter-cDNA-directed heterologous protein expression in Xenopus laevis oocytes. *Proc. Natl. Acad. Sci. USA* **89,** 1812–1816.
33. Ozaki, M., Hashikawa, T., Ikeda, K., et al. (2002) Degeneration of pontine mossy fibres during cerebellar development in weaver mutant mice. *Eur. J. Neurosci.* **16,** 565–574.

14

Receptor Knock-Out and Gene Targeting

Generation of Knock-Out Mice

Ichiro Sora, Kazutaka Ikeda, and Yuji Mishina

1. Introduction

Until recently, opioid receptors were studied only by a pharmacological approach because agonists and antagonists were the only tools available *(1)*. Interpretation of the experimental data was complicated because of the poor selectivity of opioid compounds. The precise contribution of each receptor to the effects of opioid drugs remained to be elucidated.

Gene knock-out technology, to generate a mouse with a null mutation in each opioid receptor, is one of the most important advances in studying the function of opioid receptors in vivo. Gene knock-out technology makes it possible to analyze the function of each opioid receptor with no influence of other receptor systems *(2–8)*. This chapter demonstrates the manipulation of embryonic stem (ES) cell following a previous chapter for isolation of genomic clones and another series for construction of targeting vectors. We also describe generation of chimeric mice from ES cells and analyze phenotypes for the knock-out mice involved. Because of the complexity of the techniques involved in targeting to cells, we suggest that readers examine another volume in this series *Gene Knock-out Protocols (9)*, and a further textbook *(10)* for more extensive coverage and fuller details.

2. Materials

2.1. Equipment

1. Tissue culture incubator and hood with ultraviolet (UV) light.
2. Inverted microscope.
3. Fluorometer (Pharmacia-Hoefer, DyNA count 200).

From: *Methods in Molecular Medicine, Vol. 84: Opioid Research: Methods and Protocols*
Edited by: Z. Z. Pan © Humana Press Inc., Totowa, NJ

4. Electroporation apparatus (Bio-Rad Gene pulsar, #165-2105).
5. Electroporation cuvettes (Bio-Rad, #165-2088).
6. Mouse ear puncher and ear metal tags (International Market Supplies).

2.2. Tissue Culture Reagents

1. Embryonic stem (ES) cells.
2. Feeder cells (mitotically inactivated fibroblast cells).
3. Leukemia inhibitory factor (LIF, Gibco, #13275-019).
4. β-mercaptoethanol (Sigma, #M-7522).
5. Lyophilized mitomycin C (MMC, Sigma M-0503, 2 mg/bottle).
6. Phosphate-buffered saline (PBS, Gibco, #14190-250).
7. Fetal bovine serum (FBS) (*see* **Note 1**).
8. Dulbecco's modified Eagle's medium (DMEM, Gibco, #10556-016).
9. Trypsin-ethylenediaminetetraacetate (EDTA, Gibco, #25200-056).
10. STO medium (500 mL): mix in 5 mL of 100X Penicillin-streptomycin, 5 mL of 100X glutamine-200 m*M*, 35 mL of FCS, and 455 mL of DMEM.
11. ES medium (500 mL): mix in 5 mL of 100X penicillin-streptomycin, 5 mL of 100X L-glutamine-200 m*M*, 5 mL of 100X β-mercaptoethanol, 75 mL of FBS, 500,000 U of LIF, and 410 mL of DMEM.
12. ES cell lysis buffer: 10 m*M* Tris-HCl, pH 8.0, 10 m*M* sodium chloride, 10 m*M* EDTA, 0.5% Sarcosyl, and 1 mg/mL proteinase K.
13. Restriction enzyme cocktail (per plate): 300 µL of 10X enzyme buffer, 300 µL of 10 m*M* spermidine, 150 µLof 10 U/µL restriction enzyme, and 2.25 mL of water.
14. G418 sulfate (Geneticin, Gibco, #11811-031).
15. Gancyclovir (Cyovene, Syntex).

3. Methods

3.1. Manipulation of ES Cells

Pluripotency of ES cells can be maintained by culturing them on feeder cell layers with the addition of LIF (*see* **Fig. 1**). A gene targeting construct is introduced, using electroporation, into the genome of ES cells via homologous recombination. Positive-negative selection is used to enrich targeting events. Stringent culture conditions are required to maintain the pluripotency of ES cells. Prolonged periods of culture or exposure of exhausted medium affects the ability of ES cells to contribute to the mouse germline.

3.1.1. Preparation of Fibroblast Feeder Cells from Stocks

Primary embryonic fibroblast (EMFI) cells or STO fibroblast cell lines are most commonly used as feeder layers in maintaining pluripotency of ES cells. It is best to use the same type of feeder cells as those on which the ES cells was originally established. Feeder cells must be resistant to selective reagents for screening of targeting events (e.g., G418). The following protocols are for the STO fibroblast cell line.

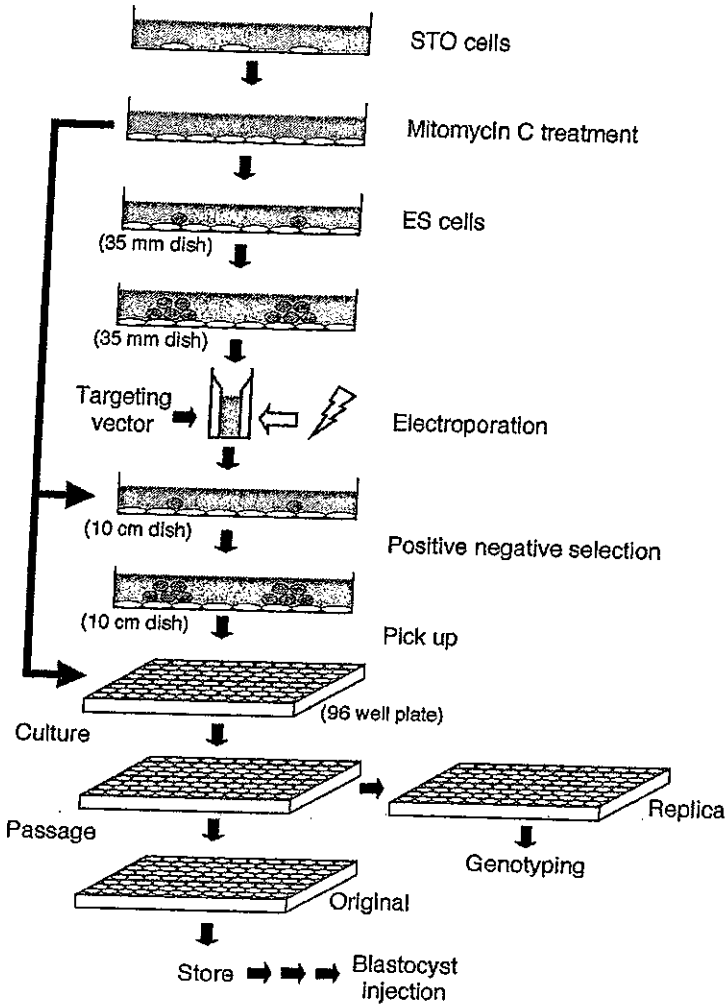

Fig. 1. Schematic illustration of procedure for screening of recombinant ES cells. ES cells are cultured on the feeder cells prepared from STO cells. The targeting vector is introduced in the ES cells by electroporation. The ES cell colonies resistant against positive-negative selection are picked up and cultured on the 96-well plates. Replicas of the 96-well plates are screened for analysis of genotype; the originals are frozen to await the results. After genotyping, correctly targeted clones are expanded to make frozen vials for blastocyst injection.

1. Put 0.1% gelatin in culture dishes and stand at room temperature at least for 1 h (gelatinized dish).
2. Remove frozen STO cell vials from the liquid nitrogen tank (5×10^6 cells) and transfer to 37°C water bath to thaw (1–2 min). Sterilize the outside of the vials with 70% ethanol.
3. Transfer the cell suspension to a sterile 15-mL tube by a transfer pipet.
4. Add 5 mL of STO medium, and centrifuge at 270*g* for 5 min. During centrifuging, remove the gelatin solution from the dishes.
5. Aspirate off the supernatant, resuspend the cell pellet in 2 mL of STO medium, and plate out the cells on a gelatinized 35-mm dish.

6. Change the medium every 3 d until STO cell become confluent.
7. Transfer to gelatinized dishes with dilution of 8 or 10 (one 35-mm dish to three 6-cm dishes, and so on).
8. When the passage number reaches 30, begin again from new frozen stock.

3.1.2. Preparation of Mitomycin C (MMC) Treated Fibroblast Feeder Layers

1. Add 4 mL of PBS to the bottle of lyophilized MMC to dissolve it. The final concentration is 0.5 mg/mL. Store at 4°C. Wear gloves for your protection from MMC toxicity.
2. Add 1/50 vol of 0.5 mg/mL freshly prepared MMC to STO medium (STO-MMC medium).
3. Aspirate medium from the dishes that have STO cells and add STO-MMC medium, then incubate for 2 h at 37°C (6 mL for 10-cm dish, 2 mL for 6-cm dish).
4. Trypsinize cells for 5 min at 37°C and make up 35 mL suspension with STO medium.
5. Take 10 µL and count the cell number with a hemacyto meter.
6. Centrifuge at 270*g* for 5 min and aspirate off the supernatant.
7. Add a sufficient amount of STO medium to the pellet to make 3.5×10^5 cells/mL suspension.
8. Distribute the suspension to gelatinized dishes. These will be ready for use within 6 h.

3.1.3. Thawing of ES Cells

In general, cells should be frozen slowly and thawed quickly. ES cells can be frozen in a freezing medium containing DMSO as a cryoprotectant. It is important to thaw the cells rapidly and remove the DMSO-containing medium as soon as possible.

1. Remove vials from liquid nitrogen tank and transfer to 37°C water bath to thaw (1–2 min).
2. Sterilize the outside of the vials with 70% ethanol.
3. Transfer the cell suspension to a sterile 15-mL tube using a transfer pipet.
4. Add 5 mL of ES medium and centrifuge at 270*g* for 5 min.
5. Aspirate off the supernatant and resuspend the cell pellet in 2 mL of ES medium.
6. Plate out the cells on a 35-mm dish having feeder cells.

3.1.4. Passage of ES Cells

1. Check ES cells under a microscope. If ES cells are 70–80% confluent, it is time for passage.
2. Refeed them and wait 2 h.
3. Remove medium and wash twice with PBS.
4. Add trypsin and incubate for 10 min at 37°C. (0.5 mL for 6 cm, 1 mL for 10-cm dish)
5. Add equal volume of ES medium to stop the reaction, and pipet up and down

10–15 times to make single cells.
6. Remove STO medium from feeder dishes and add appropriate volume of ES medium. (4 mL for 6 cm, 12 mL for 10-cm dish).
7. Add appropriate volume of ES cell suspension (*see* **Note 2**).

3.1.5. Freezing of ES Cells

1. Trypsinize cells and make up 10 mL suspension with ES medium.
2. Take 10 µL and dilute 10-fold with ES medium, then count the cell number with a hematocyto meter.
3. Centrifuge at 270*g* for 5 min and aspirate off the supernatant.
4. Add sufficient amount of ES medium to the pellet to make 1×10^7 cells/mL.
5. Add an equal amount of 2 × freezing medium dropwise to make final cell density 5×10^6. (2 × freezing medium; 60% DMEM, 20% FBS, 20% DMSO, mix in this order and prepare freshly.)
6. Distribute into sterile freezing vials (0.5 mL or 1 mL/vial) and place in Nalgen freezing container.
7. Store the container at –80°C overnight, then transfer to the liquid nitrogen tank.

3.1.6. Electroporation of DNA into ES

A linealized targeting vector is mixed with a suspension of ES cells in an apparatus that delivers electrical current (*see* **Fig. 1**). After electroporation, ES cells are plated onto *Neo*-resistant feeders with G418 for positive selection and with Gancyclovir for negative selection. The appropriate concentration of G418 for different ES cell lines must be determined by performing kill curves (usually somewhere between 150–350 µg/mL).

1. Trypsinize ES cells to make PBS suspension at 1.1×10^7 cells/mL.
2. Put 25 µL of linealized targeting vector DNA solution to a 0.4-cm cuvet.
3. Transfer 925 µL of cell suspension to the cuvet.
4. Set up the electroporation apparatus (e.g., 0.23 kV, 500 µF for Bio-Rad Gene pulsar).
5. Start the electroporation apparatus and monitor time constant (*see* **Note 3**).
6. Leave the cuvet at room temperature for 3 min, then transfer the cells in the cuvet tube to make up 30 mL with ES medium (without selection drugs).
7. Distribute the cell suspension in six 10-cm dishes of MMC-treated feeder cells (5-mL dish). Add 7 mL of ES medium (without selection drugs) to each dish to make a total medium volume of 12 mL.
8. From the next day, refeed each day with ES medium containing G418 (150–350 µg/mL) and Gancyclovir (2 m*M*).
9. Pick up colonies 10–14 d later.

3.1.7. Screening Colonies with Homologous Targeting Events

On the 10–14th d after electroporation, ES cell clones should reach picking size. Typically, 100–300 ES clones need to be analyzed to identify a handful of targeted events.